Chapter III

Finite Volume Method

The two-dimensional continuum multi-objective topology optimization in heat conduction, elastic, and thermo-elastic are employed as test problems, of which objectives of a problem are evaluated by finite volume method (FVM), in this thesis.

The FVM was originally developed for computational fluid dynamics (CFD). It is easy to understand and emphasize on direct physical interpretation [54]. In the calculation, the domain is divided into a number of non-overlapping control volumes which contain a node each. Piecewise profiles expressing the variation of a parameter ϕ between the nodal points are used to estimate the integrals in conservative law. So that the differential equation can be integrated over control volumes in order to obtain the discretized equations of a set of values of the parameter ϕ. The discretized equation satisfies the conservation principle for ϕ for any divided control volume. The finite volume method (FVM) contribute solutions that satisfy the integral conservation of quantities – such as mass, momentum, and energy – over the divided control volumes, and hence guarantees the conservation over the whole calculation domain, even though the domain is coarsely divided [54], [55].

Although the FVM was originally developed for CFD, it can be used for heat transfer [56] and elastic problems [57]. This thesis employs the FVM for simple heat conduction, linear-elastic and thermo-elastic test cases. The FVM for heat conduction problems will be described in the following topic, followed by the linear-elastic and thermo-elastic problems.

3.1. Heat Conduction Problems

A mathematical governing equation of energy conservation of a point in a two-dimensional x-y domain for a steady-state heat conduction problem is given by the following equation.

$$\frac{\partial}{\partial x}\left(k\frac{\partial T}{\partial x}\right)+\frac{\partial}{\partial y}\left(k\frac{\partial T}{\partial y}\right)+S=0 \tag{3.1}$$

where k is heat conduction coefficient, T is temperature, and S is generated heat source per unit volume of the point.

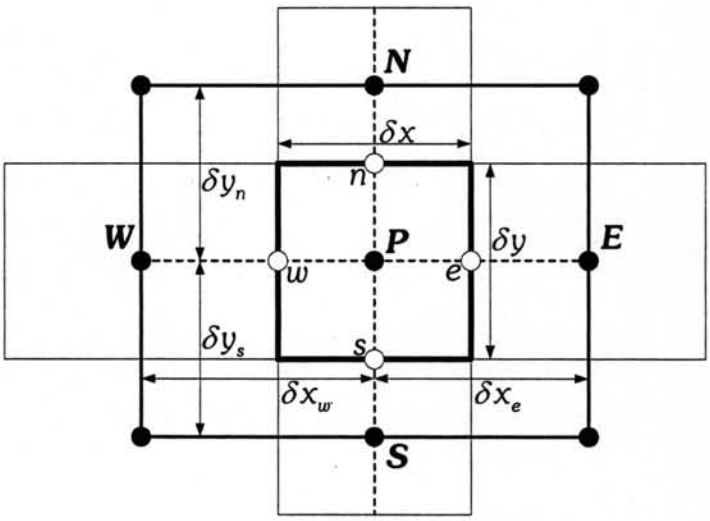

Figure 3.1 A typically control volume P.

The finite volume method (FVM) discretizes the domain into finite control volumes then the continuous space is replaced by the finite control volumes. Figure 3.1 shows a typical rectangular control volume P with uniform thickness t. The control volume P is represented by a node P at the center. The control volume P is surrounded by control volumes W, E, S, and N, which connect to the control volume P by faces w, e, s, and n, respectively. In the following equation, subscripts W, E, S, N, w, e, s, and n indicate the location of the quantity. After integrating the equation (3.1) over this control volume, the resulting integral is as follows.

$$\int \frac{\partial}{\partial x}\left(k\frac{\partial T}{\partial x}\right)dV + \int \frac{\partial}{\partial y}\left(k\frac{\partial T}{\partial y}\right)dV + \int S dV = 0 \tag{3.2}$$

By substituting $dV = tdxdy$, assuming the average value of S over the control volume as $\bar{S}$ and integrating the above equation, the resulting equation (3.3) is obtained.

$$\int_{\Delta V} \frac{\partial}{\partial x}\left(k\frac{\partial T}{\partial x}\right)tdxdy + \int_{\Delta V} \frac{\partial}{\partial y}\left(k\frac{\partial T}{\partial y}\right)tdxdy + \int_{\Delta V} Stdxdy = 0$$

$$\left[\left(k\frac{\partial T}{\partial x}\right)_e A_e - \left(k\frac{\partial T}{\partial x}\right)_w A_w\right] + \left[\left(k\frac{\partial T}{\partial y}\right)_n A_n - \left(k\frac{\partial T}{\partial y}\right)_s A_s\right] + \bar{S}\Delta V = 0 \tag{3.3}$$

where the cell surfaces $A_w = A_e = t(\delta y)$, $A_s = A_n = t(\delta x)$, and cell volume $\Delta V = t(\delta x)(\delta y)$. The first gradient term, $(k\partial T/\partial x)_e$, can be simply estimated from two nearest points of the face e in x-direction, P and E, while the other gradient terms are similarly evaluated. After substituting the approximated gradient terms, the equation becomes

$$\underbrace{-k_e A_e \frac{(T_P - T_E)}{\delta x_e}}_{Q_e} \underbrace{- k_w A_w \frac{(T_P - T_W)}{\delta x_w}}_{Q_w} \underbrace{- k_n A_n \frac{(T_P - T_N)}{\delta y_n}}_{Q_n} \underbrace{- k_s A_s \frac{(T_P - T_S)}{\delta y_s}}_{Q_s} + \underbrace{\bar{S}\Delta V}_{Q_h} = 0 \tag{3.4}$$

The first four terms in the above equation represent Q_e, Q_w, Q_n, and Q_s – heat fluxes directing out of the control volume on faces e, w, n and s – respectively, while the fifth term, Q_h, is generated heat in the control volume. The heat fluxes can be schematically displayed in Figure 3.2.

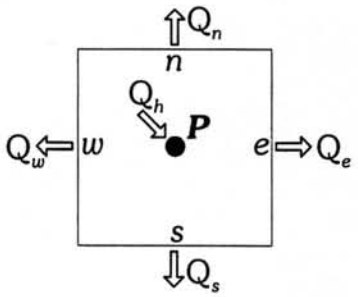

Figure 3.2 Heat fluxes on a control volume P.

By approximating $\bar{S}\Delta V$ in linearized form $\bar{S}\Delta V = S_u + S_P T_P$, expanding the equation (3.4), and rearranging terms, the resulting equation is

$$a_P T_P - a_W T_W - a_E T_E - a_S T_S - a_n T_n = S_u \tag{3.5}$$

where $$a_W = \frac{k_w A_w}{\delta x_w},\ a_E = \frac{k_e A_e}{\delta x_e},\ a_S = \frac{k_s A_s}{\delta y_s},\ a_N = \frac{k_n A_n}{\delta y_n},$$

and $$a_P = a_W + a_E + a_S + a_N - S_P \tag{3.6}$$

In addition, temperatures at faces w, e, s and n (Figure 3.1) are evaluated by linear interpolation with their neighboring nodes as the following equations.

$$T_w = \frac{|wW| T_P + |wP| T_W}{\delta x_w},\ \text{where } |wW| + |wP| = \delta x_w$$

$$T_e = \frac{|eE| T_P + |eP| T_E}{\delta x_e},\ \text{where } |eE| + |eP| = \delta x_e$$

$$T_s = \frac{|sS| T_P + |sP| T_S}{\delta x_s},\ \text{where } |sS| + |sP| = \delta x_s$$

$$T_n = \frac{|nN| T_P + |nP| T_S}{\delta x_n},\ \text{where } |nN| + |nP| = \delta x_n \tag{3.7}$$

where $|wW|$ is the length of line segment between points w and W (Figure 3.1), $|wP|$ is the length of line segment between points w and P, and so on.

The boundary implementations are described using the east surface of node P as an example (Figure 3.3). The 3 boundary conditions of problems employed in this thesis are specified temperature, specified heat flux, and convective surfaces, which can be described as follows.

1) Specified Temperature

Temperature profile along the boundary surface e in Figure 3.3 is given, thus the temperature at a point A or T_A (= T_e) on the surface is known. The heat flux out of the control volume on this boundary is simply calculated as

$$Q_A = -k_A A_A \frac{(T_P - T_A)}{\delta x_A} \tag{3.8}$$

The heat flux Q_A is substituted into the equation (3.4) as the term Q_e, and the discretized equation of the control volume is then evaluated in the same way as previous process.

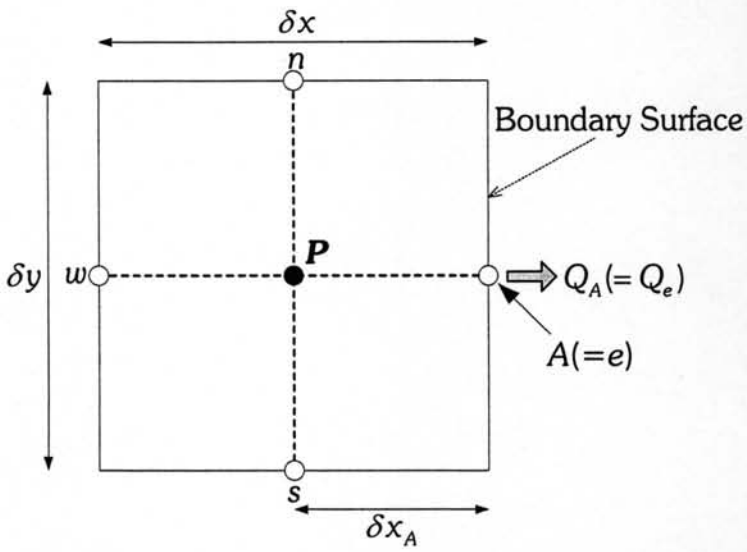

Figure 3.3 Boundary surface of a control volume *P*.

2) Specified Heat Flux

The heat flux profile along the boundary surface *e* is known (Figure 3.4), thus the resulting heat flux along the boundary face Q_A can be evaluated by the equation (3.9).

$$Q_A = -\int_{S_A} q dS \tag{3.9}$$

After the heat flux on boundary surface, Q_A, is obtained and substituted into the equation (3.4) as Q_e, the temperature at *A* or T_A can be then estimated by rearranging the equation (3.8).

$$T_A = T_P + \frac{Q_A \delta x_A}{k_A} \tag{3.10}$$

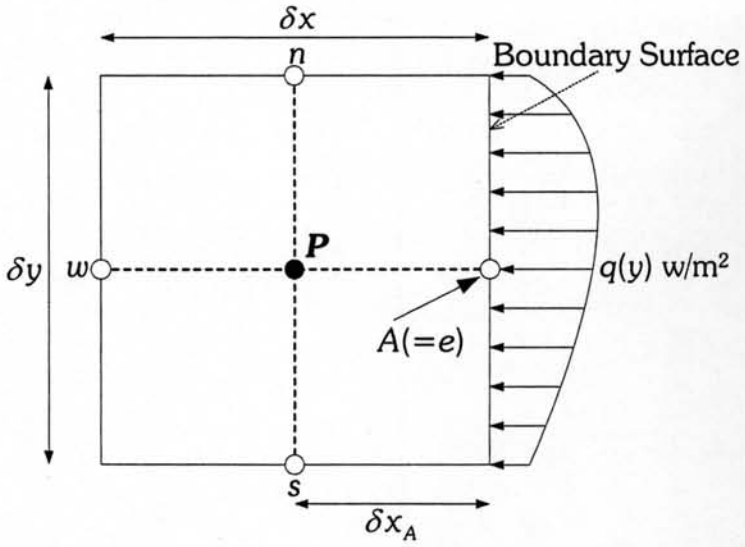

Figure 3.4 Heat source surface.

3) Convective Surface

The ambient fluid at temperature T_∞ flows along the boundary surface e with heat convection coefficient h as shown Figure 3.5. The heat flux Q_A, convection heat flux, is calculated as the following equation.

$$Q_e = Q_A = hA_A(T_A - T_\infty) \tag{3.11}$$

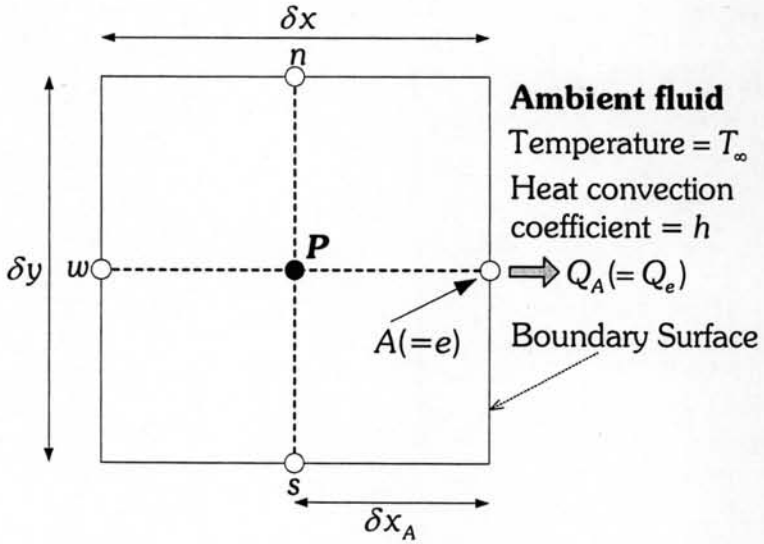

Figure 3.5 Convectional heat surface.

Due to the heat conservation, heat conducted from point P to point A (3.8) and the heat loss from point A to the ambient fluid are equal, the

temperature at point A or T_A (3.11) can be simply estimated by equaling theses two terms, resulting in the following equation.

$$T_A = \frac{h(\delta x_A)T_\infty + 2kT_P}{h(\delta x_A) + 2k} \tag{3.12}$$

3.2. Linear-Elastic and Thermo-Elastic Problems

Stress components at a point in the linear elastic material is given by

$$\begin{aligned}
\sigma_{xx} &= 2\mu\frac{\partial u}{\partial x} + \lambda\left(\frac{\partial u}{\partial x} + \frac{\partial v}{\partial y} + \frac{\partial w}{\partial z}\right) - (2\mu + 3\lambda)\alpha(\Delta T) \\
\sigma_{yy} &= 2\mu\frac{\partial v}{\partial y} + \lambda\left(\frac{\partial u}{\partial x} + \frac{\partial v}{\partial y} + \frac{\partial w}{\partial z}\right) - (2\mu + 3\lambda)\alpha(\Delta T) \\
\sigma_{zz} &= 2\mu\frac{\partial w}{\partial z} + \lambda\left(\frac{\partial u}{\partial x} + \frac{\partial v}{\partial y} + \frac{\partial w}{\partial z}\right) - (2\mu + 3\lambda)\alpha(\Delta T), \\
\sigma_{xy} &= \mu\left(\frac{\partial u}{\partial y} + \frac{\partial v}{\partial x}\right),\ \sigma_{xz} = \mu\left(\frac{\partial u}{\partial z} + \frac{\partial w}{\partial x}\right),\ \sigma_{yz} = \mu\left(\frac{\partial v}{\partial z} + \frac{\partial w}{\partial y}\right)
\end{aligned} \tag{3.13}$$

where μ and λ are Lame's coefficients, α is linear thermal expansion coefficient and ΔT is temperature change at the node.

In a two-dimensional problem, there are only three non-zero independent stress components in x and y directions, σ_{xx}, σ_{xy}, and σ_{yy} which are described as follows.

$$\begin{aligned}
\sigma_{xx} &= 2\mu\frac{\partial u}{\partial x} + \lambda\left(\frac{\partial u}{\partial x} + \frac{\partial v}{\partial y}\right) - [3K\alpha(\Delta T)] \\
\sigma_{yy} &= 2\mu\frac{\partial v}{\partial y} + \lambda\left(\frac{\partial u}{\partial x} + \frac{\partial v}{\partial y}\right) - [3K\alpha(\Delta T)] \\
\sigma_{xy} &= \sigma_{yx} = \mu\left(\frac{\partial u}{\partial y} + \frac{\partial v}{\partial x}\right)
\end{aligned} \tag{3.14}$$

It is noted that the terms in square brackets represent thermal stress components, if there is no change of temperature in the domain, these terms are equal to zero.

The Lame's coefficients are related to the shear modulus G, the Young's modulus E, Poission's ratio ν and the bulk modulus K of a plane strain problem as follows.

$$\mu = G = \frac{E}{2(1+\nu)},\ \lambda = \frac{\nu E}{(1+\nu)(1-2\nu)},\ 3K = 2\mu + 3\lambda = \frac{E}{1-2\nu} \tag{3.15}$$

For a plane stress problem, the parameters λ and K in above equation are changed as follows.

$$\lambda = \frac{\nu E}{1-\nu^2},\ 3K = \frac{E}{1-\nu} \tag{3.16}$$

In a steady-state two-dimensional problem, equilibrium equations in x, and y components are written in integral forms as follows.

x direction: $$\int_S \left(\sigma_{xx} n_x + \sigma_{xy} n_y\right) dS + \int_V \rho f_{bx} dV = 0$$

y direction; $$\int_S \left(\sigma_{yx} n_x + \sigma_{yy} n_y\right) dS + \int_V \rho f_{by} dV = 0 \tag{3.17}$$

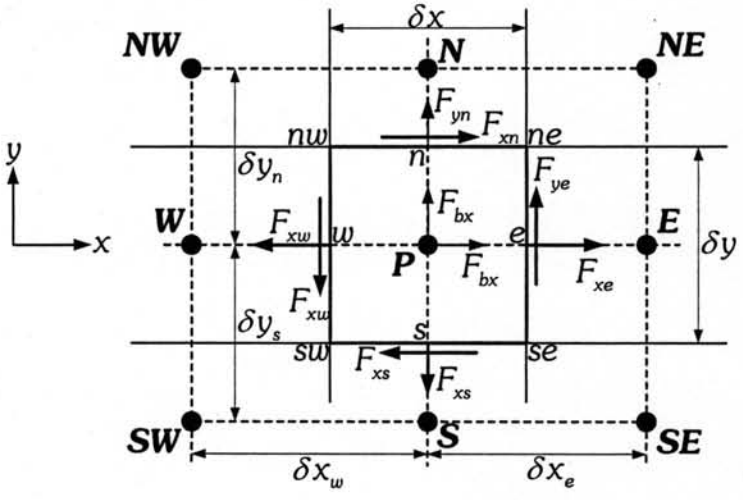

Figure 3.6 Forces acting on a control volume P.

The unit directional vector components $[n_x, n_y]$ of surfaces w, e, s, and n (Figure 3.6) are [-1,0], [1,0], [0,-1], and [0,1], respectively. By substituting these directional components, equation (3.17) becomes

$$x \text{ direction: } \underbrace{\int_{S_e} \sigma_{xx} dS}_{F_{xe}} - \underbrace{\int_{S_w} \sigma_{xx} dS}_{F_{xw}} + \underbrace{\int_{S_n} \sigma_{xy} dS}_{F_{xn}} + \underbrace{\int_{S_s} \sigma_{xy} dS}_{F_{xs}} + \underbrace{\int_V \rho f_{bx} dV}_{F_{bx}} = 0$$

$$y \text{ direction: } \underbrace{\int_{S_e} \sigma_{yx} dS}_{F_{ye}} - \underbrace{\int_{S_w} \sigma_{yx} dS}_{F_{yw}} + \underbrace{\int_{S_n} \sigma_{yy} dS}_{F_{yn}} - \underbrace{\int_{S_s} \sigma_{yy} dS}_{F_{ys}} + \underbrace{\int_V \rho f_{by} dV}_{F_{by}} = 0 \tag{3.18}$$

The forces in equation (3.18) can be geometrically explained in Figure 3.6. By substituting stress components in equations (3.14) and areas of faces *e*, *w*, *n*, and *s* – A_e, A_w, A_n, and A_s – the discretized forms of forces on a control volume *P* [58] are obtained as follows.

x direction:

$$F_{xw} = \int_{S_w} \left(2\mu \frac{\partial u}{\partial x} + \lambda \left(\frac{\partial u}{\partial x} + \frac{\partial v}{\partial y} \right) - \left[3K\alpha(\Delta T_w) \right] \right) dS$$

$$F_{xw} \approx 2\mu \left(\frac{u_P - u_W}{\delta x} \right) A_w + \lambda \left(\frac{u_P - u_W}{\delta x} + \frac{v_{nw} - v_{sw}}{\delta y} \right) A_w - [3K\alpha(\Delta T_w)] A_w$$

$$F_{xw} \approx \frac{(2\mu + \lambda) A_w}{\delta x} (u_P - u_W) + \frac{\lambda A_w (v_{nw} - v_{sw})}{\delta y} - \left[3K\alpha(\Delta T_w) A_w \right] \tag{3.19}$$

In the same way,

$$F_{xe} \approx \frac{(2\mu + \lambda) A_e}{\delta x} (u_E - u_P) + \frac{\lambda A_e (v_{ne} - v_{se})}{\delta y} - \left[3K\alpha(\Delta T_e) A_e \right] \tag{3.20}$$

$$F_{xs} \approx \frac{\mu A_s}{\delta y} (u_P - u_S) + \frac{\mu A_s}{\delta x} (v_{se} - v_{sw}) \tag{3.21}$$

$$F_{xn} \approx \frac{\mu A_n}{\delta y} (u_N - u_P) + \frac{\mu A_n}{\delta x} (v_{ne} - v_{nw}) \tag{3.22}$$

For body force,

$$F_{bx} = \int_V \rho f_{bx} dV$$

$$F_{bx} \approx \rho f_{bx}^P (\Delta V) \tag{3.23}$$

y direction:

$$F_{yw} \approx \frac{\mu A_w}{\delta x} (v_P - v_W) + \frac{\mu A_w}{\delta y} (u_{nw} - u_{sw}) \tag{3.24}$$

$$F_{ye} \approx \frac{\mu A_e}{\delta x}(v_E - v_P) + \frac{\mu A_e}{\delta y}(u_{ne} - u_{se}) \tag{3.25}$$

$$F_{ys} \frac{(2\mu + \lambda)A_s}{\delta y}(v_P - v_S) + \frac{\lambda A_s}{\delta x}(u_{se} - u_{sw}) - [3K\alpha(\Delta T_s)A_s] \tag{3.26}$$

$$F_{yn} \approx \frac{(2\mu + \lambda)A_n}{\delta y}(v_N - v_P) + \frac{\lambda A_n}{\delta x}(u_{ne} - u_{se}) - [3K\alpha(\Delta T_n)A_n] \tag{3.27}$$

$$F_{by} \approx \rho f_{by,P}(\Delta V) \tag{3.28}$$

By substituting the discretized forms of the forces acting on the control volume into the equilibrium equation (3.18) in x and y directions, then the equilibrium equations are discretized as follows.

x direction:

$$a_P^u u_P - a_W^u u_W - a_E^u u_E - a_S^u u_S - a_N^u u_N + \frac{\lambda A_w (v_{nw} - v_{sw})}{\delta y} - \frac{\lambda A_e (v_{ne} - v_{se})}{\delta y} + \frac{\mu A_s}{\delta x}(v_{se} - v_{sw})$$
$$- \frac{\mu A_n}{\delta x}(v_{ne} - v_{nw}) = b^u \tag{3.29}$$

where

$$a_W^u = \frac{(2\mu + \lambda)A_w}{\delta x},\ a_E^u = \frac{(2\mu + \lambda)A_e}{\delta x},\ a_S^u = \frac{\mu A_s}{\delta y},\ a_N^u = \frac{\mu A_n}{\delta y},$$
$$a_P^u = a_W^u + a_E^u + a_S^u + a_N^u$$

and
$$b^u = \rho f_{by,P}(\Delta V) + \left[3K\alpha(\Delta T_e)A_e - 3K\alpha(\Delta T_w)A_w\right] \tag{3.30}$$

y direction:

$$a_P^v v_P - a_W^v v_W - a_E^v v_E - a_S^v v_S - a_N^v v_N + \frac{\mu A_w}{\delta y}(u_{nw} - u_{sw}) - \frac{\mu A_e}{\delta y}(u_{ne} - u_{se}) + \frac{\lambda A_s}{\delta x}(u_{se} - u_{sw})$$
$$- \frac{\lambda A_n}{\delta x}(u_{ne} - u_{se}) = b^v \tag{3.31}$$

where

$$a_W^v = \frac{\mu A_w}{\delta x},\ a_E^v = \frac{\mu A_e}{\delta x}, a_S^v = \frac{(2\mu + \lambda)A_s}{\delta y},\ a_N^v = \frac{(2\mu + \lambda)A_n}{\delta y},$$
$$a_P^v = a_W^v + a_E^v + a_S^v + a_N^v$$

and
$$b^v = \rho f_{by,P}(\Delta V) + \left[3K\alpha(\Delta T_n)A_n - 3K\alpha(\Delta T_s)A_s\right] \tag{3.32}$$

If there are no temperature changes in the domain, that is no thermal stresses, terms in square brackets are equal to zero. The displacements u and v at faces w, e, s and n can be estimated by interpolating from their neighboring points as in the approximation of temperature in a heat conduction problem. Similar to the estimation of the u and v, displacement differences in the y direction – v_{nw}-v_{sw}, v_{ne}-v_{se}, v_{se}-v_{sw}, and v_{ne}-v_{nw} of face w, e, s, and n respectively in above equation (3.29) – can be simply estimated from their neighboring faces as follows.

$$
\begin{aligned}
v_{nw} - v_{sw} &= \frac{|wW|(v_n - v_s) + |wP|(v_{nW} - v_{sW})}{\delta x_w} \\
v_{ne} - v_{se} &= \frac{|eE|(v_n - v_s) + |eP|(v_{nE} - v_{sE})}{\delta x_e} \\
v_{se} - v_{sw} &= \frac{|sS|(v_e - v_w) + |sP|(v_{Se} - v_{Sw})}{\delta y_s} \\
v_{ne} - v_{nw} &= \frac{|nN|(v_e - v_w) + |nP|(v_{Ne} - v_{Nw})}{\delta y_n}
\end{aligned}
\tag{3.33}
$$

In the same way, displacement differences in the x direction – u_{nw}-u_{sw}, u_{ne}-u_{se}, u_{se}-u_{sw}, and u_{ne}-u_{nw} – are also approximately evaluated from their adjacent faces as the evaluation of the v differences in above equation (3.33).

Four boundary conditions – Dirichlet, Neumann, mixed, and symmetry plane boundary conditions [58] – are described in the following topics using the east surface as an example.

1) Dirichlet Boundary Condition

In the Dirichlet boundary condition, displacements u and v at a point A are known as shown in Figure 3.7, the forces acting at the point A, F_{Ax} and F_{Ay}, are computed as the following equation.

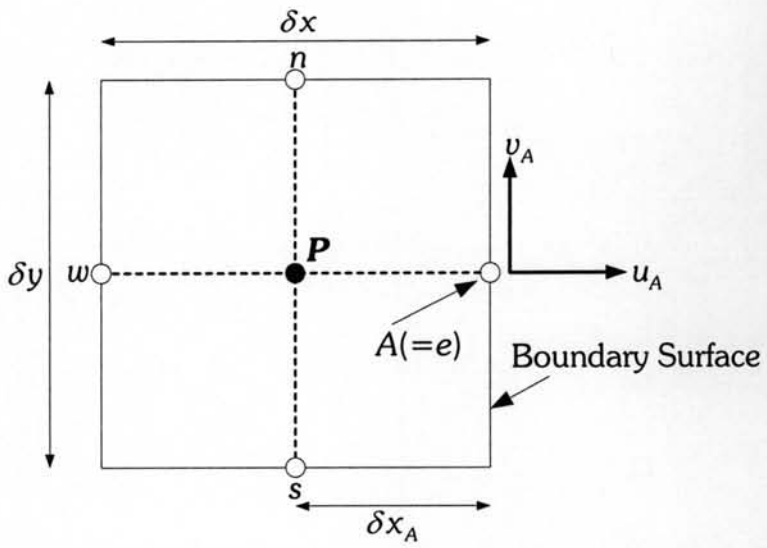

Figure 3.7 Dirichlet boundary condition.

$$F_{Ax} = \frac{(2\mu+\lambda)A_A}{\delta x_A}(u_A - u_P) + \frac{\lambda A_A(v_{An} - v_{As})}{\delta y} - [3K\alpha(\Delta T_A)A_A]$$
$$F_{Ay} = \frac{\mu A_A}{\delta x}(v_A - v_P) + \frac{\mu A_A}{\delta y}(u_{An} - u_{As}) \qquad (3.34)$$

Similar to the previous evaluation, the forces F_{Ax} and F_{Ay} in the above equation will be then substituted into the equilibrium equation (3.18), to obtain the discretized equilibrium equations in x and y directions of the control volume.

2) Neuman Boundary Condition

In the Neuman boundary conditions, the surface tractions t_{Ay} and t_{Ax} acting on the surface e are known (Figure 3.8), the forces F_{Ax} and F_{Ay} are the follows.

$$F_{Ax} = t_{Ax}A_A$$
$$F_{Ay} = t_{Ay}A_A \qquad (3.35)$$

The displacements u and v at a point A, u_A and u_B, are therefore evaluated by substituting F_{Ax} and F_{Ay} into equation (3.34).

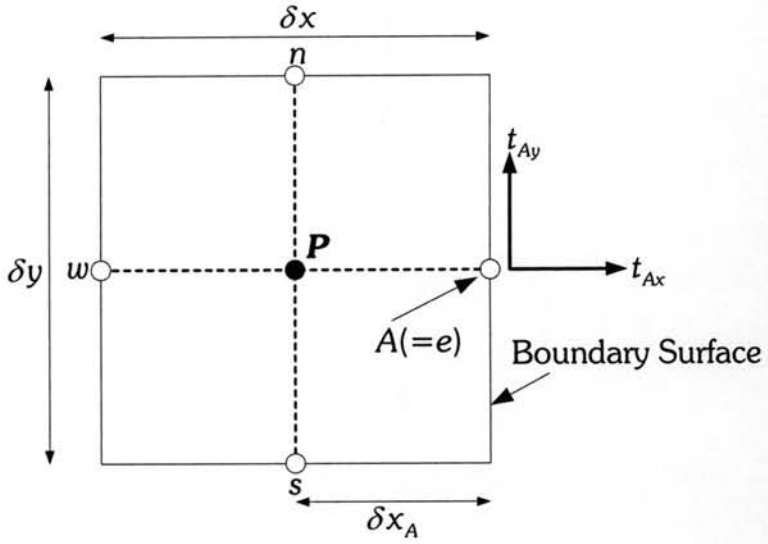

Figure 3.8 Neuman boundary condition.

3) Mixed Boundary Condition

In this boundary condition, the surface boundary consists of Dirichlet and Neumann boundary conditions in different directions. Figure 3.9 shows the example of a control volume of which boundary surface *e* has the mixed boundary condition.

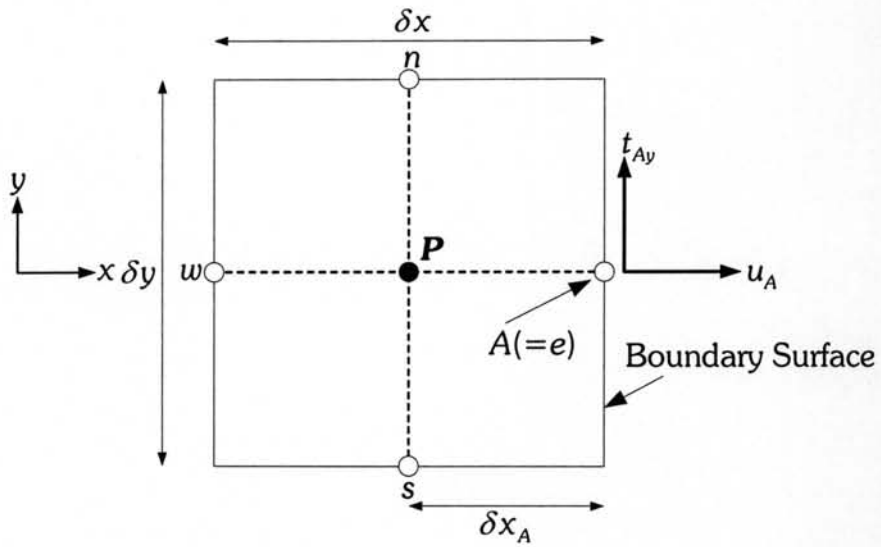

Figure 3.9 Mixed boundary condition.

On the surface, a displacement u_A, which represents the Dirichlet boundary condition, in x direction and traction t_{Ay}, which represents the Neumann boundary condition in y direction, are known. For the mixed boundary condition in Figure 3.9, the discretized equilibrium equation of Dirichlet boundary direction is derived from equation (3.34) while that of Neumann boundary direction is obtained from equation (3.35).

4) Symmetry Plane

The symmetry plane boundary condition can be shown by Figure 3.10. Therefore, displaments in x and y direction are as the following equations.

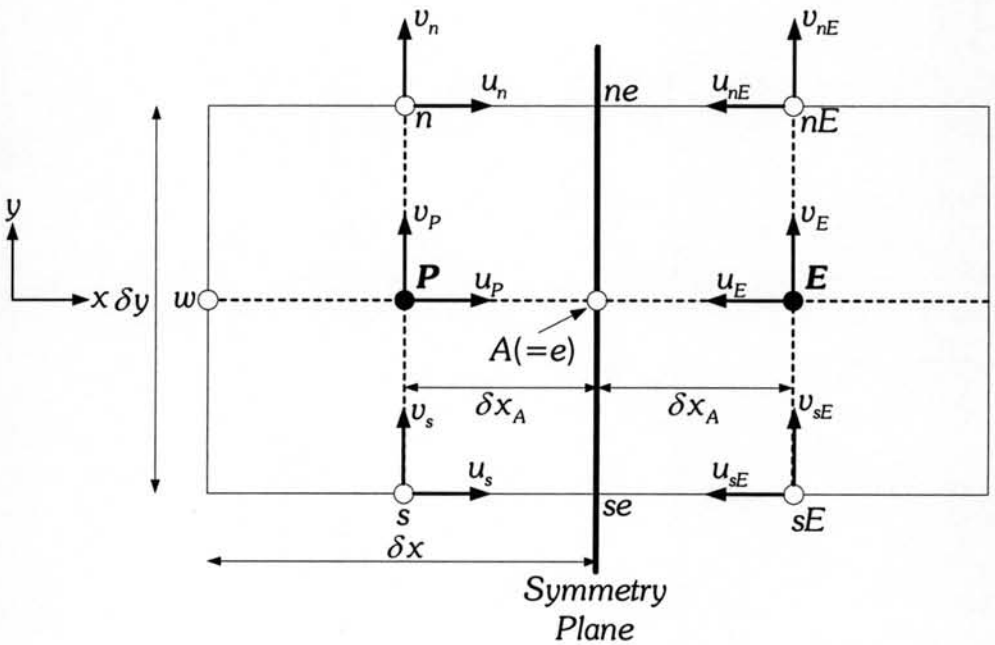

Figure 3.10 Symmetry Plane Boundary Condition.

x direction:

$$u_{nE} = -u_n,\ u_E = -u_P,$$

$$u_{ne}\text{-}u_{se} = 0.5(u_n + u_{nE})\text{-}0.5(u_s + u_{sE}) = 0 \tag{3.36}$$

y direction:

$$v_{nE} = v_n,\ v_E = v_P,\ v_{sE} = v_s \tag{3.37}$$

Due to the equality of v_E and v_P and u_{ne}-u_{se} = 0 in the above equations, subsequently by F_{ye} is equal to zero according to the equation (3.25).

3.3. Solution Algorithms

For all employed problems, after assembling discretized equations of unknown parameters of all control volumes, the system of algebraic equations is obtained. The system is solved by LU decomposition method [59], thereafter, the values of parameters of all control volume are obtained. For an employed problem, after unknown parameters of a solution, a two-dimensional structure, are obtained by the FVM. The parameters are then used to evaluate the corresponding objectives of the solution.

This chapter describes the finite volume methods (FVMs) for all employed continuum topology optimization problems – heat conduction, linear-elastic, and thermo-elastic problems. For a continuum topology optimization problem, the FVM is used to evaluate objectives of a solution, while a multi-objective evolutionary algorithm (MOEA) is used to search optimum solutions of the problem. The descriptions and simulation results of the employed continuum topology optimization problems will be drawn in Chapter V. The next chapter will present evaluation of performance of all 5 employed MOEAs – 2 well-established MOEAs and 3 proposed MOEAs – for multi-objective benchmark problems.